Arch Virol (2006) 151: 2161–2180
DOI 10.1007/s00705-006-0791-2

Archives of Virology
Printed in Austria

Ultrastructural study of myxoma virus morphogenesis

J.-L. Duteyrat, J. Gelfi, and **S. Bertagnoli**

UMR 1225 Interactions Hôtes-Agents pathogènes, INRA/ENVT, Ecole Nationale Vétérinaire de Toulouse, Toulouse, France

Received September 26, 2005; accepted April 26, 2006
Published online June 9, 2006

Summary. Poxviruses are among the largest and most complex viruses known. Vaccinia virus, the prototype of the family *Poxviridae*, has been studied much more than myxoma virus.

The aim of this work was to have a better knowledge about myxoma virus morphogenesis.

The characterization of the main stages of MV morphogenesis was achieved by ultrastructural and immunological analysis. Specific antibodies were raised against M022L and M071L, two envelope proteins of extracellular enveloped virus and intracellular mature virus, respectively. The main stages of assembly were similar to those seen with other poxviruses, and the duration of the whole replication cycle was estimated to be around 16 h, longer than what was described for vaccinia virus. Morphological changes of infected cells were associated with the development of long cellular projections and enlarged microvilli. Intracellular enveloped viruses are associated with the cytoskeleton to move through the cell. Unlike earlier studies, as many cell-associated enveloped viruses as intracellular enveloped viruses were observed in relation with specialized microvilli, although these structures were rarely noticed. Finally, an unusual spreading process was observed, which uses cytoplasmic corridors.

Introduction

The *Poxviridae* are a large family of complex DNA viruses that replicate in vertebrate and invertebrate hosts. Their genome is composed of a single linear double-stranded DNA molecule and encodes its own machinery required for both replication and transcription. Thereby, they are able to replicate and assemble in the cytoplasm of host cells. The most notorious member, variola virus, caused smallpox and consequently had a profound impact on human history. Moreover, vaccinia virus (VACV) was the first animal virus seen microscopically, grown in tissue culture, accurately titered, physically purified and chemically analysed [36].

Among the numerous poxviruses, myxoma virus (MV) is the agent of myxomatosis, a highly lethal disease of the European rabbit (*Oryctolagus cuniculus*) [17]. MV has a double-stranded DNA of 162 kbp [6], with a classical poxviral organisation, the central region encoding essential proteins, and the peripheral regions encoding nonessential factors that contribute to the modulation of the host response to infection [38]. Moreover, MV had been used as a vector for vaccination [2, 4, 34] or immunocontraception [23].

Yet, little is known about the morphogenesis of MV [41, 54, 55] compared to the extensively studied VACV maturation process [10, 13, 15, 26, 44, 46, 49, 51, 57].

The aim of this study was to have a better knowledge of the MV replication cycle and morphogenesis. The first part of this work consists of the characterization of the main stages of MV morphogenesis. This was achieved by using electron microscopy and positive staining with or without immunogold labelling.

The second part of this study focuses on the morphological modifications of infected cells during the course of the viral cycle life, and the involvement of the cytoskeleton by MV for its egress. Indeed, during the infection by MV, the infected cells showed numerous dramatic morphological modifications.

This study has allowed the determination of the main stages of assembly of MV during the viral cycle life, which are similar to those seen with VACV, and to suggests that the cytoskeleton (actin and microtubules) is used by MV for its egress. We confirm the existence and the importance of a new spreading process, using cytoplasmic corridors reminiscent of original cellular projections recently described for the MVA strain of VACV [18].

Materials and methods

Cells and virus

RK13 (rabbit kidney cells) were cultured in Dulbecco's modified Eagle medium (DMEM, Gibco) containing penicillin and streptomycin and 10% fetal calf serum (FCS). Cells were cultured at 37 °C in 5% CO_2. Infections were performed using MV strain T1 [5] at a multiplicity of infection (m. o. i.) of 8. Cells were kept on ice for 2 h to allow virus adsorption to the plasma membrane. They were then washed with minimal essential medium and incubated at 37 °C in complete medium with 2% FCS.

Antibodies

Based on the comparison between MV and VACV DNA sequences [6], M071L (H3L VACV homolog) and M022L (F13L VACV homolog) proteins were chosen as specific antigens for the IMV and EEV forms, respectively. After PCR amplification, the M022L and M071L ORFs were cloned in pTrcHis-TOPO plasmids (Invitrogen). Viral proteins were expressed in *E. coli* strain Top 10 according to the manufacturer's instructions, and purified using affinity HIS-TRAP Chelating HP columns (FPLC AKTA System, Amersham-Pharmacia Biotech). Then, 12-week-old New Zealand white rabbits were injected subcutaneously three times with 150 µg of M022L or M071L proteins and bled to give specific immune antisera. Hyper immune anti-MV serum was produced by vaccinating and challenging rabbits with MV.

Preparation of cells for transmission electron microscopy

Infected and mock-infected cells were prepared for transmission electron microscopy at 0.5, 1, 3, 8, 12, 16, 20, 24, 30, 36 and 48 h post infection (p.i.). At the indicated times, they were fixed in 2% glutaraldehyde (Electron Microscopy Sciences, Washington PA.) in 0.1 M cacodylate buffer (pH 7.4) containing 2% tannic acid [39] and 0.003 M $CaCl_2$, for 4 h at 4 °C and washed four times in 0.2 M cacodylate buffer (pH 7.4) containing 0.003 M $CaCl_2$. Then, cells were incubated for 1 h in 0.1 M cacodylate buffer (pH 7.4) containing 1% OsO_4 (SIGMA), washed several times in distilled water, then incubated for 12 h in 2% uranyl acetate and subjected to several washes in distilled water. After dehydration, monolayers were embedded using an Araldite 502/Embed 812 Kit (Electron Microscopy Sciences, Washington PA.). Sections were cut parallel to the surface of the dish and stained with 2% uranyl acetate [28] for 20 min and lead citrate for 10 min before visualization [42].

Immunogold labelling of thin sections

Cells were infected as described above and then fixed with 4% paraformaldehyde-0.1% glutaraldehyde in 0.1 M phosphate buffer (pH 7.4) for 30 min at 4 °C. Cells were then scraped from the dish, collected by centrifugation (400 × *g*), overlaid with additional fixative, washed four times with 0.2 M phosphate buffer (pH 7.4), and subjected to graded dehydration and embedded in LR White resin (medium Grade acrylic resin, Agar Scientific), which had been cured at 50 °C for 24 h.

Sections were collected on 200 mesh-gold grids. EEVs as first antigen were labelled on the upper side by rabbit anti-M022L antibody (diluted 1/50) and IMV as second antigen on the lower side of the section by rabbit anti-M071L antibody (diluted 1/50). The labelling procedure was as follows: sections were incubated with ammonium chloride (0.05 M, pH 7.8) for 10 min at room temperature (RT), blocked with 0.1% BSA-5% NGS-0.2% Tween 20 in PBS (pH 7.4) for 15 min at RT prior to being incubated for 12 h at 4 °C with the primary antiserum in blocking solution. The sections were then washed in 0.1% BSA-PBS three times for 7 min, washed in 0.1% fish skin gelatin in PBS for 5 min, and incubated for 1 h at RT with 5-nm-diameter gold (M022L) or 10-nm-diameter (M071L) bead-conjugated goat anti-rabbit immunoglobulin G (BBI). Grids were then washed in PBS, fixed for 5 min in 1% glutaraldehyde, rinsed with distilled water, and poststained with 2% uranyl acetate (aqueous) for 20 min. Grids were examined on a HITACHI HU-12A microscope.

Indirect immunofluorescent staining for confocal microscopy

At 20 h p.i., the cells were fixed with cold 4% paraformaldehyde in PBS at RT for 90 min, rinsed three times with PBS and then permeabilized with 0.1% Triton X-100 in PBS for 15 min at RT. After washing in PBS, cells were incubated with rabbit anti-MV hyperimmune serum (diluted 1/500) in 0.05% Tween 20 in PBS for 1 h at 37 °C, visualized by Cy-5-conjugated affiniPure Donkey anti-rabbit IgG (H+L) (Jackson ImmunoResearch Laboratories-Inc) (diluted 1/200). Tubulin was stained with MAb rat anti-tubulin YL (Serotec UK) (diluted 1/20), which was detected by FITC-conjugated anti-rat IgG (SIGMA) (diluted 1/200). F-actin was stained with TRITC-phalloïdin (SIGMA) (diluted 1/200). Cells were analysed using an OLYMPUS FV 500 confocal laser scanning microscope. Images were collected and processed using common fluoview software for FV 500 and Adobe Photoshop software.

Results

Characterization of different viral forms and intermediates on thin sections

Very little information is available concerning the viral life cycle of MV. We hence decided to use an electron microscopy approach to identify the viral forms and intermediates. Moreover, immunogold labelling was used as an additional tool for ultrastructural identification.

At 20 h p.i. many different viral forms and intermediates were directly observed and easily recognized (not shown): these were crescents, immature virions (IVs), intracellular mature virions (IMVs), intracellular enveloped virions (IEVs), cell-associated enveloped virions (CEVs), and extracellular enveloped virions (EEVs).

IMVs were also characterized by immunogold labeling using anti-M071L antibodies. (Fig. 1a). IVs were also labelled, the subviral localization of gold particles being mostly peripheral (Fig. 1b), just beneath or on the envelope, suggesting that this protein is added to the viral particle early during virus assembly and remains on the first envelope. Enveloped virus forms (IEVs, CEVs, EEVs) were unequivocally characterized by immunogold labelling using anti-M022L antibodies (Fig. 1 c–e). Indeed, M022L is a homologue of the vaccinia F13L protein, the most abundant enveloped virus protein [49]. The morphological identification of enveloped virus forms was easy and the labelling only confirmed the ultrastructural recognition.

Double labelling (M071L and M022L) confirmed that enveloped virus forms consist of an IMV with additional membrane(s) (Fig. 1f, g). In Fig. 1g, the wrapping membrane cisterna is clearly labelled by anti-M022L. This implies that this envelope protein is already inserted into the wrapping compartment before the wrapping of IMVs.

Ultrastructural morphogenesis study of MV during the replication cycle

In order to measure the duration of the virus life cycle, we determined the main stages of the assembly of MV by electron microscopy. Rabbit kidney cells (RK13) were infected with MV strain T1 at a m.o.i. of 8, then harvested at different times for conventional electron microscopy analysis.

The virus life cycle can be divided into two phases: an early phase (from adsorption to eclipse) and a late phase (post-eclipse stage) where the morphogenetic structures become obvious.

At 0 h p.i., viral particles were observed in close association with the plasma membrane (Fig. 2a). Just after adsorption, viral particles penetrated the cell. In Fig. 2b, a viral particle seems to penetrate the cell, membrane fragments are obvious at the plasma membrane, and we noticed the continuity between the inner viral and the plasma membranes. These fragments could correspond to the outer viral membrane, which could be disrupted during adsorption and/or penetration. Sometimes, EEVs were surrounded by microvilli, as if phagocytosis had occurred (Fig. 2c). An invagination of the plasma membrane could also be seen where EEVs penetrated the cell (Fig. 2d).

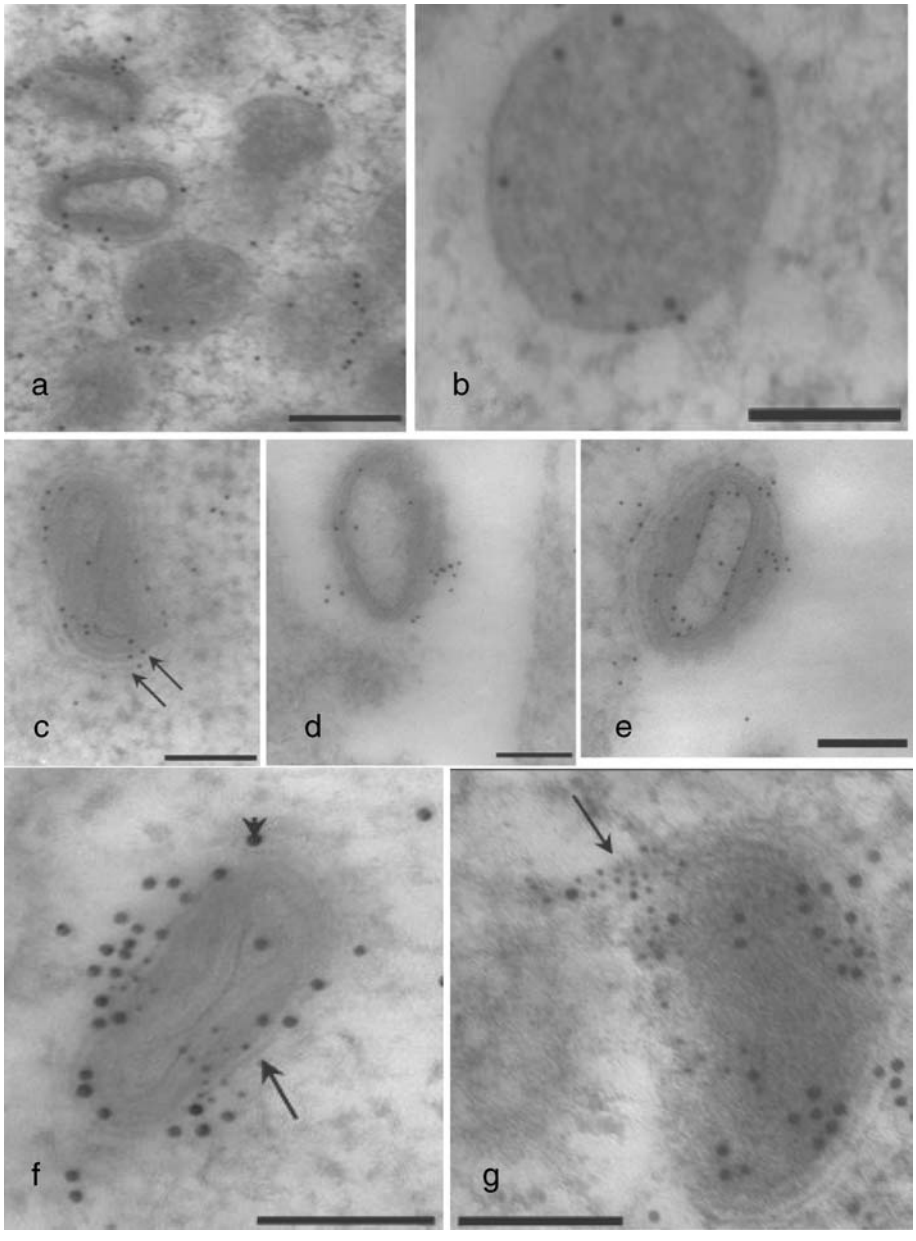

Fig. 1. Immunogold labelling of MV on thin sections. **a** Localisation of the majority of labelling (anti-M071L) on the surface of the IMV particles. **b** Labelling (anti-M071L) of IV particles (mostly peripheral). **c** IEV labelled with anti-M022L antibodies (arrows point to outer viral membranes). **d** EEV particle labelled with anti-M022L antibodies. **e** CEV particle labelled with anti-M022L antibodies. **f** Double labelling of an IEV particle: M022L detected by gold beads of 5 nm (arrow); M071L detected by gold beads of 10 nm (arrowhead). **g** Labelling of the wrapping membrane cisterna of the IMV (arrow). Bars, 200 nm (a); 100 nm (b–g)

At 30 min p.i., numerous particles were seen in the cytoplasm. Some of them lay within a vesicle formed at the cell surface (presumably by invagination). Inside the vesicle the outer viral membrane was obvious, either intact or partly damaged

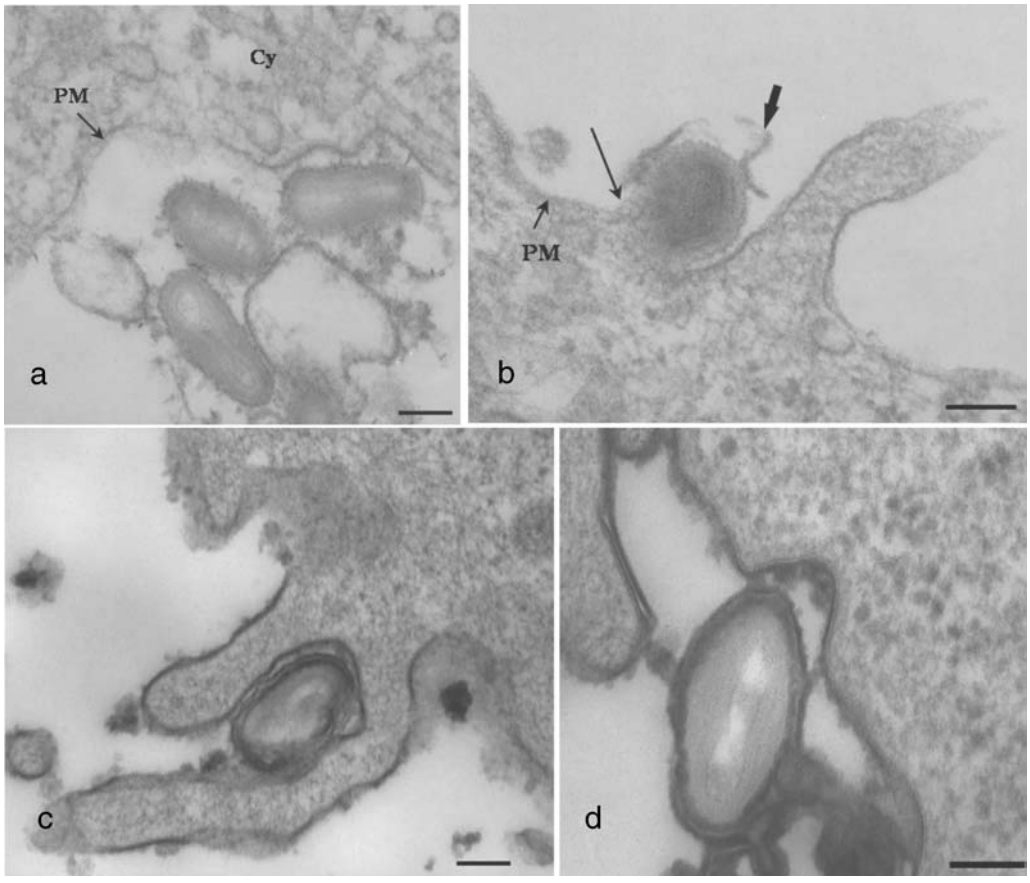

Fig. 2. Adsorption and penetration of MV (0 h p.i.). **a** Adsorption of three viral particles to the plasma membrane; *Cy* cytoplasm; *PM* plasma membrane. **b** A viral particle penetrating the cell. Large arrow: viral membrane fragments. We can see the continuity between the plasma membrane (*PM*) and the inner viral membrane (thin arrow). **c** An EEV particle is being phagocytosed. **d** Apparent invagination of the plasma membrane where the viral particle (EEV) penetrates. In **c** and **d**, potassium ferricyanide was used to enhance the cell membrane [16]. Bars, 100 nm

(Fig. 3a). However, from this time until late stages of morphogenesis, most viruses were clustered into large vesicles (Fig. 3b, c). Simultaneously, numerous uncoating figures were noticed (Fig. 3d–f), sometimes near the nuclear envelope (Fig. 3f), implying that uncoating occured rapidly.

From the beginning of the eclipse phase (3 h p.i.) until 8 h p.i., numerous myelin-like figures, consisting of concentric multilamellar structures, were seen (Fig. 3g).

Assembly began with the formation of discrete membranes at 8 h p.i.. Sometimes tangential or oblique sections of portions of the shell clearly showed a multilaminar membrane (Fig. 4a). Depending on the section, subunits, reminiscent of spicules, covered the external side of the membrane (Fig. 4b).

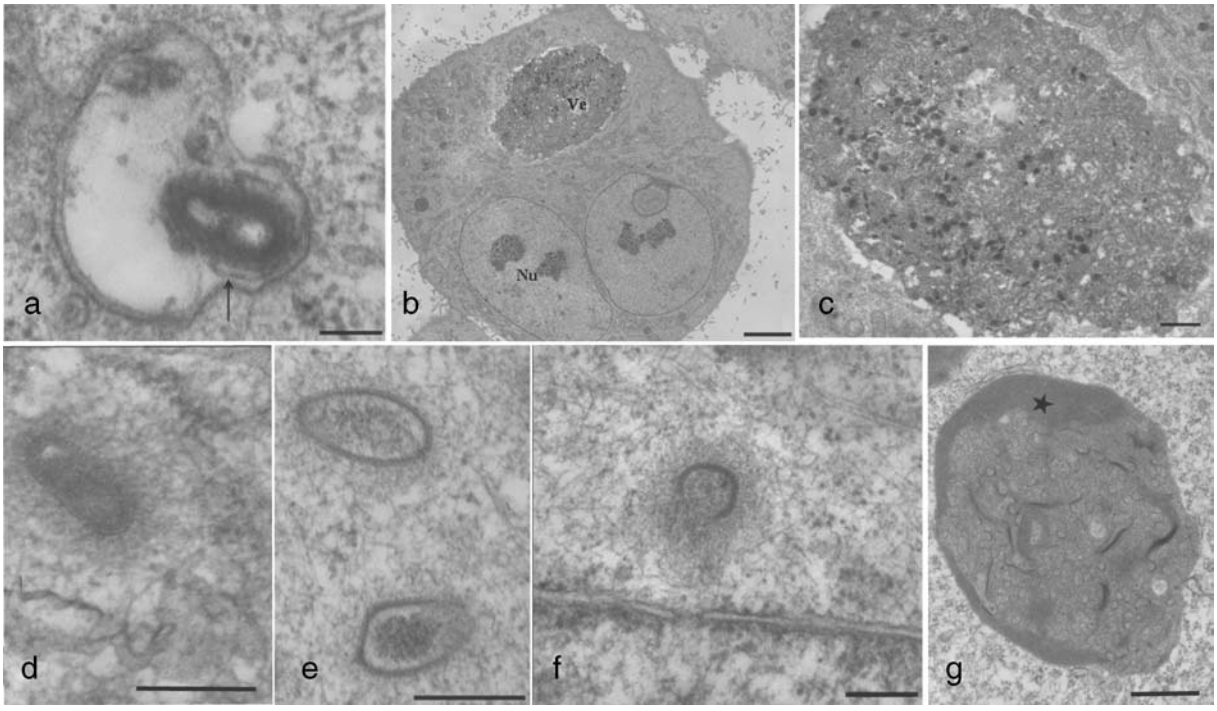

Fig. 3. Early stages of the viral life cycle. **a** The outer viral membrane is partly damaged (arrow) inside a vesicle presumably formed at the cell surface (30 min p.i.). **b** Most viruses are clustered into large cytoplasmic vesicles (*Ve*) from 30 min p.i. until later stages of infection (*Nu* nucleus). At a higher magnification **c** numerous electron-dense viral particles (30 min p.i.). **d** First stage of disassembly where the viral envelope is still distinguishable (30 min p.i.). **e** Later stage of uncoating: only the viral core is still apparent (30 min p.i.). **f** Last stage of uncoating just before the disappearance of the viral core into the cytoplasm (1 h p.i.). **g** Myelin-like figures in the cytoplasm (3 h p.i.). They consist of concentric multilamellar structures (star). Bars, 100 nm (a); 4 μm (b); 1 μm (c); 200 nm (d–f); 500 nm (g)

The first morphologically distinct structures were crescent-shaped structures consisting of a membrane with a brush-like border of spicules on the convex surface and granular material adjacent to the concave side. At the end of these structures, loops were sometimes obvious (Fig. 4c). Some observations suggest that there is a continuity between the crescent envelope and long membrane structures (Fig. 4d). These appeared around electron-dense areas of cytoplasm called viroplasm foci. Tangential or oblique sections of the crescent revealed the presence of faint lattice lines (Fig. 4e). Such lattice lines could be a product of random hexagonal packing of the surface subunits [35, 53]. Numerous vesicular elements could remain in the vicinity of crescents, sometimes linked to them or around factories (Fig. 4f). These crescents then developed into spherical immature virions (IVs), either tightly apposed to the nuclear membrane or surrounded by a cell compartment (probably the smooth endoplasmic reticulum) (not shown). IVs had either achieved the condensation of their nucleoid (Fig. 4h), or had just been penetrated by DNA before sealing (Fig. 4g).

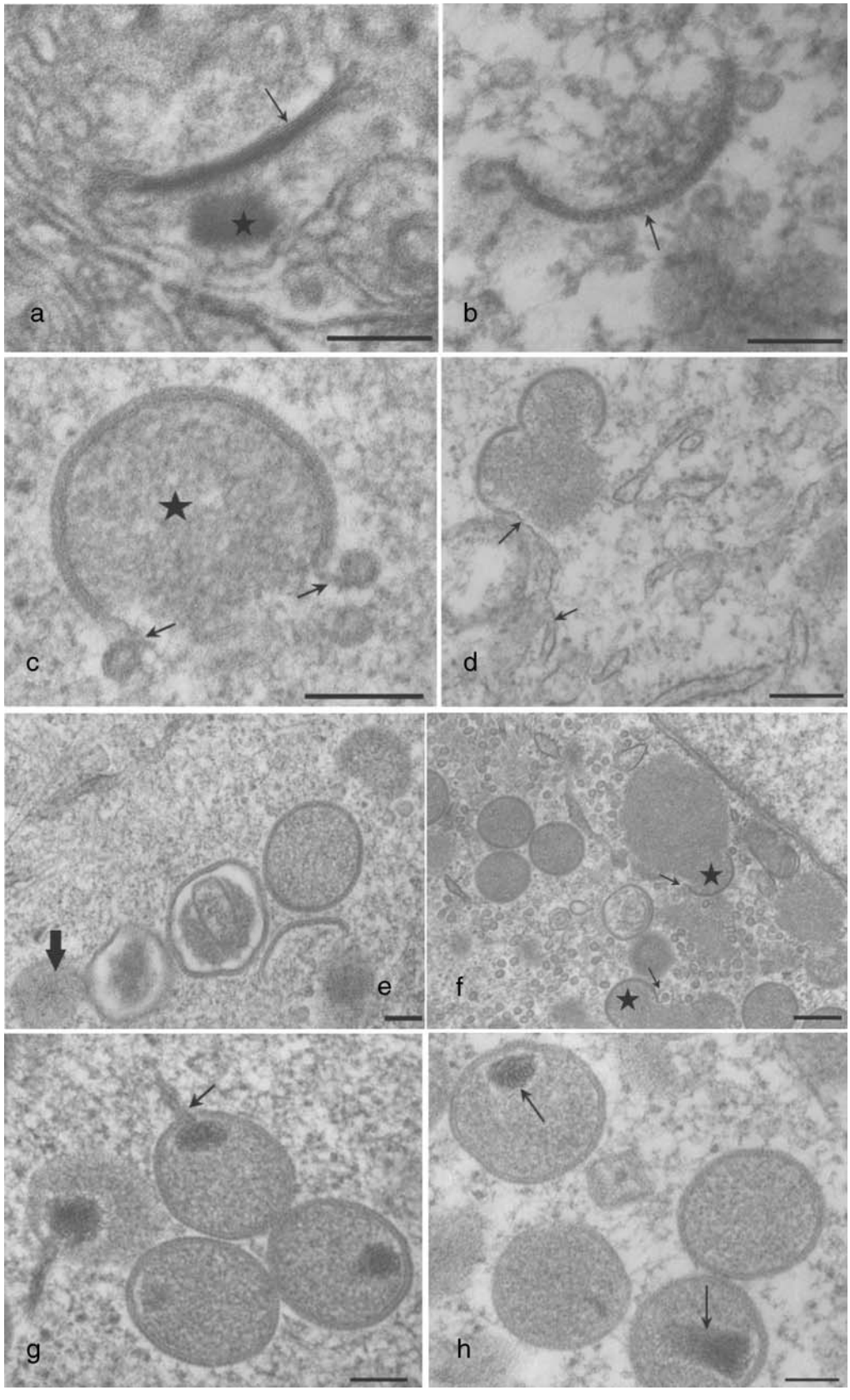
a
b
c
d
e
f
g
h

IVs then matured into brick-shaped particles called intracellular mature virions (IMVs), following the classical steps of maturation (not shown). At 12 h p.i., IMVs were wrapped by a membrane cisterna, either alone (Fig. 5a) or associated (Fig. 5b), generating intracellular enveloped viruses (IEVs) (Fig. 5e). Some observations suggest that this wrapping membrane cisterna could be the rough endoplasmic reticulum (RER) (Fig. 5c), others the Golgi apparatus (Fig. 5d). Numerous IEVs are stacked near the plasma membrane (Fig. 5f) just before their release.

Extracellular enveloped viruses (EEVs) are formed when the outer membrane fuses with the plasma membrane. They were either released from the cell or retained at the cell surface as cell-associated enveloped viruses (CEVs). From 16 h p.i., electron-dense striated areas of cytoplasm were obvious in factories near newly formed IVs (Fig. 5g). At a higher magnification, the crystal network was evident (Fig. 5h), reminiscent of the nucleoid inside the IVs. From 20 h p.i., there was a marked increase in the rate of CEV formation. Taken together, these results suggest that MV morphogenesis follows the classical stages of poxviral morphogenesis, the MV replication cycle taking place in approximately 16 h (Table 1). We also confirmed these kinetics by a single-step growth curve analysis on RK13 cells (data not shown), consistent with growth curves obtained using other permissive cell cultures [27].

Exit of MV from the cell: specialized microvilli and cytoplasmic corridor

Knowing that cytoskeletal changes occur during the exit of the virus from the cell, we first studied the relationship between the cytoskeleton and the enveloped virus forms by transmission electron microscopy.

At 20 h p.i., microtubules were often closely associated with IEVs near the plasma membrane (Fig. 6a, b), suggesting their role in the intracellular movements of IEVs. Actin fibers sometimes formed bundles surrounding an IEV, to which they seemed to be attached (Fig. 6c). An extensive ultrastructural observation allowed visualizing specialized microvilli, corresponding to actin tails, used for egress. Either CEVs (Fig. 6d, e) or IEVs (Fig. 6i) were associated with these microvilli. However, this association was not a frequent event. Sometimes IEVs

Fig. 4. Early stages of morphogenesis (8 h p.i.). **a** Tangential (star) or oblique (arrow) sections of discrete viral membranes at 8 h p.i.. **b** Section of the discrete viral membrane reveals external subunits (arrow). **c** Crescent-shaped structures (star shows the granular material on the concave side; arrow shows the loops). **d** Apparent continuity between the crescent envelope and a long membranous structure (arrow). **e** Tangential sections of immature viruses (IVs) reveal faint lattice lines (large arrow). **f** Numerous little vesicles remain in the factories, sometimes linked to crescents (arrows); stars show granular material. **g** DNA just enters before sealing of the IV (arrow). **h** Condensation of nucleoid in the IV (arrow). Bars, 100 nm (a–c, e, g, h); 200 nm (d); 250 nm (f)

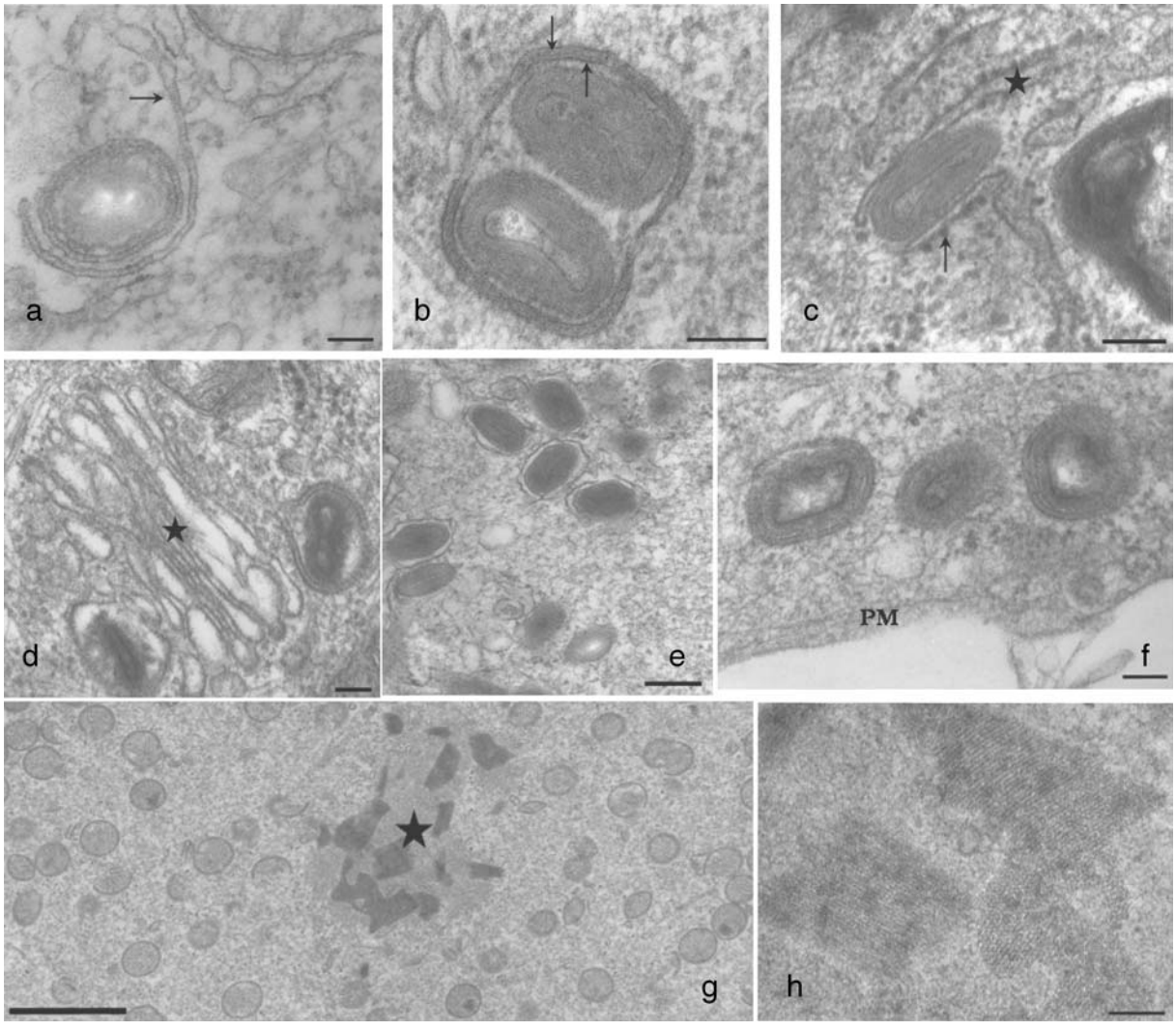

Fig. 5. Wrapping of IMVs (12 h p.i.) by a membrane cisterna to form IEVs. **a** Wrapping of a single IMV particle (arrow: cisterna appearance). **b** Two particles wrapped together (arrows: the two membrane profiles). **c** A wrapping membrane cisterna could be part of the rough endoplasmic reticulum (star, arrow focuses on the ribosomes). **d** Two IMV particles are surrounded by two Golgi cisternae (star, Golgi apparatus). **e** IEVs in the cytoplasm clearly show the outer membrane cisterna. **f** Numerous IEVs near the plasma membrane before release (*PM* Plasma Membrane). **g** Later during infection, some electron-dense striated areas in the factories (star). **h** The crystal network, characteristic of the viral DNA, at a higher magnification. Bars, 100 nm (a–d, f, h); 205 nm (e); 1 μm (g)

clearly labelled by M022L were obvious inside a long cellular projection (Fig. 6f–h). The projections did not always have a precise direction (Fig. 6f).

We also used confocal microscopy to complete the study of MV spreading. We did not see the typical actin tails, but frequently observed cytoplasmic projections connecting several neighbouring cells, delimited by the plasma membrane (red)

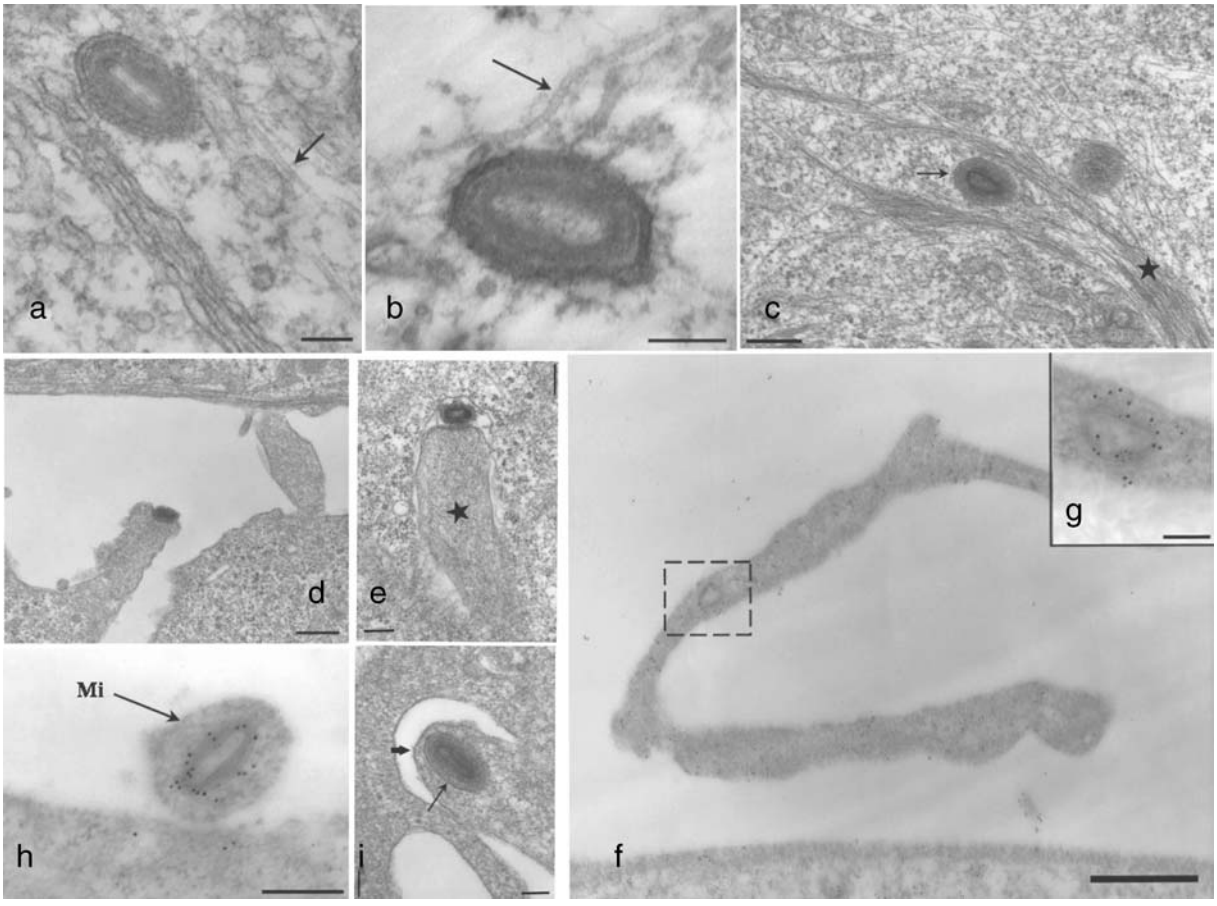

Fig. 6. MV uses the cytoskeleton for its egress (TEM). **a** An IEV is shown next to a microtubule (arrow). **b** A microtubule seems to be linked to the viral particle (arrow). **c** IEV particle encompassed by an actin bundle (star). The two membrane profiles (arrow) are very clear. **d** A CEV particle at the top of a microvillus. **e** A CEV particle at the top of a microvillus (star) which has penetrated a neighbouring cell. **f**, **g** An IEV particle labelled by anti-M022L (magnification, Bar 100 nm) is clearly distinct in the cell projection. **h** A transversal section of a microvillus (arrow, Mi, Microvillus) containing an IEV. **i** An IEV at the top of a microvillus. The membrane of the microvillus is shown by a large arrow, the two-membranes profile, which characterizes the IEV particle, is indicated by the thin arrow. Bars, 250 nm (a, c, e, h); 100 nm (b, g, i); 0.5 μm (d); 1 μm (f)

and containing viruses (blue) (Fig. 7a). No discontinuity was observed between these cytoplasmic corridors and the cells. We refined these observations using TEM: late during infection, a few ruffled cellular projections containing viral particles were seen (Fig. 7b). A cytoplasmic deck was observed between two cells, which formed a corridor allowing viral particles to progress towards neighbouring cells (Fig. 7c).

Our observations, generated using different techniques, indicate a close relationship between IEVs/CEVs, actin, and microtubules, leading to different spreading processes.

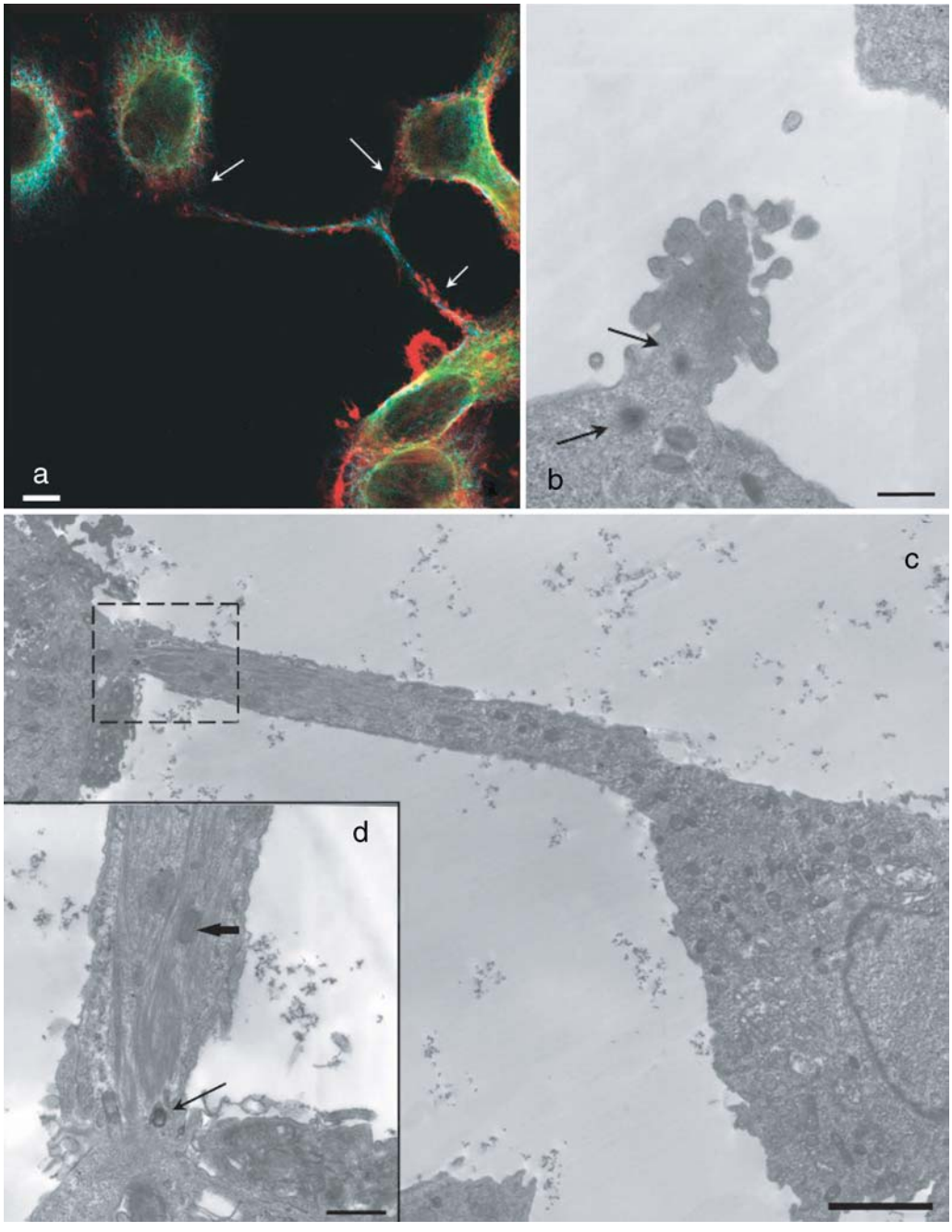

Fig. 7. MV uses cytoplasmic corridors for its egress. **a** A cytoplasmic corridor links three cells (arrows) (confocal microscopy). Blue: viruses in this structure; red: the plasma membrane; green: microtubules. **b** Ruffled microvilli containing several viral particles (arrows), which could correspond to the first stage of the building of this cytoplasmic corridor (TEM). **c** A cytoplasmic corridor containing viral particles and linking two cells. **d** An IEV particle is clearly observed in this structure (large arrow) and a CEV on the top of it (thin arrow). Bars, 4 μm (a); 0.5 μm (b, d); 3 μm (c)

Table 1. Schematic comparison between the MV and VACV replication cycles

Stages of viral cycle	Adsorption	Penetration	Eclipse phase	Morphogenesis stages	
MV	*0 h* viral particles in close association with plasma membrane	*30 min p.i.*; particles in cytoplasmic vesicles; numerous uncoating figures	*3 h–8 h p.i.*; numerous myelin-like figures in the cytoplasm; viral factories	*from 8 h p.i.*; discrete viral membranes Crescent IVs IMVs	*from 12 h p.i.*; IEVs *from 16 h p.i.;* CEVs and EEVs *from 20 h p.i.*; Marked increase of CEVs
VACV	viral particles in close association with plasma membrane	uncoating occurs rapidly (few minutes after penetration)	*20 min–2 h p.i.;* viral factories appear at 3 h p.i.	*from 3 h p.i.*; Crescents *from 4 h p.i.*; IVs *from 7 h p.i.*; IMVs	*8 h–12 h p.i.;* IEVs, then CEVs and EEVs

Discussion

This article is the first complete report dealing with the morphogenesis and the egress of a leporipoxvirus, although Tektoff et al. [54] presented one of the first real ultrastructural observations of MV. The aim of our study was to have a better knowledge about the morphogenesis and replication cycle of MV. Little is known about the morphogenesis of MV compared to the extensively studied Vaccinia virus (VACV) maturation process. Therefore, we systematically compared MV to VACV, the prototype of the family *Poxviridae*.

The first part of this work consisted of the recognition and identification of the viral forms and intermediates by ultrastructural and immunological analysis. This was completed by a dynamic analysis of the viral cycle.

At 20 h p.i., all of the different viral forms and intermediates were observed. IMVs and EEVs were characterised by using antibodies against M071L and M022L, proteins homologous to the VACV envelope proteins H3L and F13L, respectively [6]. After checking the specificity of the labelling on purified isolated particles (data not shown), single and double labelling were used on thin sections. The double labelling allowed enveloped and non-enveloped virus forms to be distinguished more clearly on the same section.

We focused on the different stages of the viral life cycle. Adsorption could be determined by the observation of a physical link between viral particles and the cell surface. The entry process is very fast, therefore rarely visualized. Numerous particles were seen in the cytoplasm at 30 min p.i.. Some of them lay within a vesicle formed at the cell surface, presumably by invagination, as previously described for VACV EEV entry [59]. Particles were clearly surrounded by microvilli reminiscent of phagocytosis. Sometimes, it seemed that the EEV inner virus membrane and the

plasma membrane fused, the outer viral membrane remaining at the cell surface. In fact, the manner in which poxviral particles penetrate the cell is still a matter of discussion [30]. It has been speculated that actin redistribution induced by IMV entry is similar to the initial stages of phagocytosis, since IMVs are theoretically large enough to induce a phagocytic response [32].

The fusion process has been described elsewhere [7, 8, 14]. Although the early stages of viral entry were very rarely seen, our observations seem to favour endocytosis and/or phagocytosis. It should be interesting to study these interactions more precisely, to modify the experimental methods (high concentration of virus or spinoculation), and to specifically label IMVs and EEVs [7].

From 1 to 3 h p.i., most viral particles were clustered in large cytoplasmic vesicles. These were previously considered to be an abortive phenomenon [11] leading to viral degradation. However, for the inocula used in our studies, the calculated ratio of infectious particles to non-infectious particles was 1/10, which is not consistent with a massive degradation of defective viruses. Thus, these vesicles could result from the engulfment of numerous particles, taken up all at once by the cell. This phenomenon, known as macropinocytosis, has sometimes been described for viruses [31, 33, 48] and even more often for bacteria [3, 40, 56]. A fraction of the virions that are internalized into intracellular vesicles could escape destruction by preventing their delivery to lysosomes. Their survival within phagosomes would lead to productive infection [33, 40]. This process is in accordance with the possibility of a silent entry of EEVs [32], thus not triggering cellular defence mechanisms.

During the eclipse phase, some myelin-like figures have been described. Some authors have argued for a hypothetical artefact due to the use of tannic acid [39, 47]. We compared our results in the absence or presence (not shown) of tannic acid, and these characteristic images were observed under both experimental conditions. It has been proposed that they originate from lipid granules [1], and could represent a lipid supply for the generation of virus envelopes.

The first newly-formed viral structures appearing at 8 h p.i., were crescent-shaped structures. They consist of a membrane with a brush-like border of spicules on the convex surface and granular material adjacent to the concave side [35]. They appear around electron-dense areas of cytoplasm called viroplasm foci [44]. Then, the crescents develop into spherical immature virions (IVs) in which condensation of nucleoid occurs. In MV morphogenesis, the presence of M071L protein was detected during the early stages of assembly (IVs), suggesting an essential role in the building of IMVs.

We saw a relationship between crescent and membrane structures, and later, between IVs and a cell compartment. This is in accordance with Sodeik et al. [51], who suggested that vaccinia virus membranes are not synthesized *de novo*, but derive from the intermediate compartment of the host cell. Since no cell compartment was labelled by anti-M071L antibodies, the nature of the cell membranes is unclear. The number of membranes surrounding an IMV particle is disputed [7, 10, 20, 21, 25, 29, 44, 51, 52], and our observations cannot really support a

particular model. Nevertheless, the numerous observations of little vesicles near factories and IVs could favour the two-membranes theory. These vesicules have been observed with mutant VACV that are unable to produce IMVs [57]. Here, the same accumulation of vesicles was observed with a wild-type MV. In agreement with previous studies, we can imagine that vesicles could represent a normal event in the maturation process, a normal intermediate in the biogenesis of viral particles. These numerous little vesicles could fuse to form a membrane cisterna which represents the first viral membrane. This cisterna could then collapse and mimic a "one-membrane-only" profile, corresponding to two tightly apposed bilayers. Parallel to these observations, we mostly noticed that loops existed at the ends of crescents or viral membranes: these could correspond to the ends of collapsed membrane cisternae [51].

From 12 to 16 h post infection, some IMVs became wrapped by a cell compartment, not clearly identified in our study, but probably the RER or Golgi apparatus, to form IEVs. According to different studies, IMVs are wrapped in a double layer of membrane derived from either the trans Golgi network (TGN) [46] or endosomes [58]. At this time point, the cisternae wrapping membrane was clearly labelled with anti-M022L antibodies before being around the viral particle. This indicates that M022L protein is associated with this membrane cisterna before wrapping.

At this time, egress happened and proceeded rather by exocytosis. No budding was observed. IEVs move to the cell surface where the outer membrane fuses with the plasma membrane, forming CEVs retained at the cell surface, or EEVs released from the cell [49].

During the later stages of virus morphogenesis we noticed electron-dense striated areas of cytoplasm thought to be DNA crystalloid. These structures could be generated in the presence of drugs [22], or with mutants [12], which was not the case here.

A few long linear ladder structures, presumably of lipidic origin, accumulated concomitantly (not shown). Their implication in virus morphogenesis is not known [13].

We decided to use confocal microscopy and TEM to determine if MV manipulates the cytoskeleton as VACV does (for a review, see [50]). With confocal microscopy there was no difference in microtubule distribution between infected and mock-infected cells (data not shown), in accordance with previous observations by Hollinshead et al. [24]. However, a cytoplasmic deck, containing viral particles, connected neighbouring cells. The cytoplasmic decks were also observed by TEM, and a few virions (IEVs), either labelled or not, were running on to infect neighbouring cells. Specialized microvilli, also named actin tails, were sometimes observed with either a CEV or an IEV on their tip.

Earlier studies on VACV suggested that both actin and microtubules were involved in egress [37, 43]. In fact, actin is thought to be responsible for the formation of specialized microvilli, and only CEVs would be able to give rise to actin polymerisation [24, 37, 43, 49, 58, 60]. Nevertheless, some authors have reported that IEVs were also able to cause the polymerisation of actin [9, 45]. It is

known that in the case of bacteria [19, 56], actin tail polymerisation occurs in the cytoplasm, and bacteria are pushed towards the cell in a directed manner without the bacteria being exocytosed.

Our results suggest two processes of infection using cellular projections. One, abundantly described by many authors, implies an actin-containing microvillus pushing one virus particle. Another would consist of a large cytoplasmic corridor, allowing a few virions (IEVs) to migrate and infect neighbouring cells. This particular cellular projection looks like the philopodium recently specifically described for the MVA strain of VACV [18]. Indeed, when grown in monolayers, MVA-infected semi-permissive cells connect themselves to others by using a long cellular projection.

Perhaps the association between actin and IEVs is only a transient stage before their release to form CEVs with actin bundle. On the other hand, it may be another process of cell-to-cell dissemination where IEVs remain in the cytoplasm. Then the two cell membranes could fuse at the top of the cellular projection or the cytoplasmic corridor, allowing the virus to penetrate the cell without being released and exposed to the immune response. Cytoplasmic corridors must be a frequent phenomenon, since they were more commonly observed in our study than the classical specialized microvilli by the two methods, TEM and confocal microscopy.

This study has allowed the different stages of myxoma virus assembly and the entire viral life cycle (approximately 16 h) to be visualized, and to determine how virus particles egress. We showed the existence of a unusual spreading process for MV, *i.e.* cytoplasmic corridors. In the future, immunogold labelling could help to elucidate which cell compartments are involved in the wrapping process of IMVs to form IEVs. Further investigations would permit the identification of the large cytoplasmic vacuoles containing numerous virions. Finally, it seems that MV, and more generally poxviruses, share numerous similarities with mycobacteria: the entry process, the putative capacity to survive within host cells after being internalized in cytoplasmic vacuoles, and the use of the cytoskeleton for their egress.

Acknowledgments

We are grateful to Josyane Loupias and Brigitte Péralta for excellent technical assistance. Special thanks to Danielle Spehner and Robert Drillien for critical review of the manuscript.

We dedicate this article to the memory of Frédérique Messud.

References

1. Arhelger RB, Randall CC (1964) Electron microscopic observations on the development of fowlpox virus in chorioallantoic membrane. Virology 22: 59–66
2. Barcena J, Morales M, Vazquez B, Boga JA, Parra F, Lucientes J, Pages-Mante A, Sanchez-Vizcaino JM, Blasco R, Torres JM (2000) Horizontal transmissible protection against myxomatosis and rabbit hemorrhagic disease by using a recombinant myxoma virus. J Virol 74: 1114–1123

3. Barker LP, George KM, Falkow S, Small PL (1997) Differential trafficking of live and dead mycobacterium marinum organisms in macrophages. Infect Immunol 65: 1497–1504
4. Bertagnoli S, Gelfi J, Le Gall G, Boilletot E, Vautherot JF, Rasschaert D, Laurent S, Petit F, Boucraut-Baralon C, Milon A (1996) Protection against myxomatosis and rabbit viral hemorrhagic disease with recombinant myxoma viruses expressing rabbit hemorrhagic disease virus capsid protein. J Virol 70: 5061–5066
5. Bouvier G (1954) Quelques remarques sur la myxomatose. Bull Off Int Epizoot 46: 76–77
6. Cameron C, Hota-Mitchell S, Chen L, Barrett J, Cao JX, Macaulay C, Willer D, Evans D, McFadden G (1999) The complete DNA sequence of myxoma virus. Virology 264: 298–318
7. Carter GC, Law M, Hollinshead M, Smith GL (2005) Entry of the vaccinia virus intracellular mature virion and its interactions with glycosaminoglycans. J Gen Virol 86: 1279–1290
8. Chang A, Metz DH (1976) Further investigations on the mode of entry of Vaccinia virus into cell. J Gen Virol 32: 275–282
9. Cudmore S, Reckmann I, Way M (1997) Viral manipulations of the actin cytoskeleton. Trends Microbiol 5: 142–148
10. Cyrklaff M, Risco C, Fernandez JJ, Jimenez MV, Esteban M, Baumeister W, Carrascosa JL (2005) Cryo-electron tomography of vaccinia virus. Proc Natl Acad Sci USA 102: 2772–2777
11. Dales S (1973) Poxviruses. In: Dalton AJ, Haguenau F (eds) Ultrastructure of animal viruses and bacteriophages: an atlas. Vol 5. Academic Press, New York, pp 109–129
12. Dales S, Milovanovitch V, Pogo BG, Weintraub SB, Huima T, Wilton S, McFadden G (1978) Biogenesis of vaccinia: Isolation of conditional lethal mutants and electron microscopic characterization of their phenotypically expressed defects. Virology 84: 403–428
13. Dales S, Mosbach EH (1968) Vaccinia as a model for membrane biogenesis. Virology 35: 564–583
14. Doms RW, Blumenthal R, Moss B (1990) Fusion of intra- and extracellular forms of vaccinia virus with the cell membrane. J Virol 64: 4884–4892
15. Dubochet J, Adrian M, Richter K, Garces J, Wittek R (1994) Structure of intracellular mature vaccinia virus observed by cryoelectron microscopy. J Virol 68: 1935–1941
16. Elbers PF, Ververgaert PH, Demel DJ (1965) Tricomplex fixation of phospholipids. J Cell Biol 24: 23–30
17. Fenner F, Ratcliffe F (1965) Myxomatosis. Cambridge University Press, Cambridge
18. Gallego-Gomez JC, Risco C, Rodriguez D, Cabezas P, Guerra S, Carrascosa JL, Esteban M (2003) Differences in virus-induced cell morphology and in virus maturation between MVA and other strains (WR, Ankara, and NYCBH) of vaccinia virus in infected human cells. J Virol 77: 10606–10622
19. Gouin E, Welch MD, Cossart P (2005) Actin-based motility of intracellular pathogens. Curr Opin Microbiol 8: 35–45
20. Griffiths G, Roos N, Schleich S, Locker JK (2001a) Structure and assembly of intracellular mature vaccinia virus: thin-section analyses. J Virol 75: 11056–11070
21. Griffiths G, Wepf R, Wendt T, Locker JK, Cyrklaff M, Roos N (2001b) Structure and assembly of intracellular mature vaccinia virus: isolated-particle analysis. J Virol 75: 11034–11055

22. Grimley PM, Rosenblum EN, Mims SJ, Moss B (1970) Interruption by rifampin of an early stage in vaccinia virus morphogenesis: accumulation of membranes which are precursors of virus envelopes. J Virol 6: 519–533
23. Holland MK, Jackson RJ (1994) Virus-vectored immunocontraception for control of wild rabbits: identification of target antigens and construction of recombinant viruses. Reprod Fertil Dev 6: 631–642
24. Hollinshead M, Rodger G, Van Eijl H, Law M, Hollinshead R, Vaux DJ, Smith GL (2001) Vaccinia virus utilizes microtubules for movement to the cell surface. J Cell Biol 154: 389–402
25. Hollinshead M, Vanderplasschen A, Smith GL, Vaux DJ (1999) Vaccinia virus intracellular mature virions contain only one lipid membrane. J Virol 73: 1503–1517
26. Husain M, Moss B (2003) Evidence against an essential role of COPII-mediated cargo transport to the endoplasmic reticulum-Golgi intermediate compartment in the formation of the primary membrane of vaccinia virus. J Virol 77: 11754–11766
27. Johnston JB, Nazarian SH, Natale R, McFadden G (2005) Myxoma virus infection of primary human fibroblasts varies with cellular age and is regulated by host interferon responses. Virology 332: 235–248
28. Knight DP (1977) Staining Methods in electron microscopy. Glauert; Cambridge, pp 40–47
29. Krijnse-Locker J, Schleich S, Rodriguez D, Goud B, Snijder EJ, Griffiths G (1996) The Role of a 21-kDa viral membrane protein in the assembly of vaccinia virus from the intermediate compartment. J Biol Chem 271: 14950–14958
30. Law M, Smith GL (2004) Studying the binding and entry of the intracellular and extracellular enveloped forms of vaccinia virus. Methods Mol Biol 269: 187–204
31. Liu NQ, Lossinsky AS, Popik W, Li X, Gujuluva C, Kriederman B, Roberts J, Pushkarsky T, Bukrinsky M, Witte M, Weinand M, Fiala M (2002) Human immunodeficiency virus type 1 enters brain microvascular endothelia by macropinocytosis dependent on lipid rafts and the mitogen-activated protein kinase signaling pathway. J Virol 76: 6689–6700
32. Locker JK, Kuehn A, Schleich S, Rutter G, Hohenberg H, Wepf R, Griffiths G (2000) Entry of the two infectious forms of Vaccinia virus at the plasma membrane is signaling-dependent for the IMV but not the EEV. Mol Biol Cell 11: 2497–2511
33. Marechal V, Prevost MC, Petit C, Perret E, Heard JM, Schwartz O (2001) Human immunodeficiency virus type 1 entry into macrophages mediated by macropinocitosis. J Virol 75: 11166–11177
34. McCabe VJ, Tarpey I, Spibey N (2002) Vaccination of cats with an attenuated recombinant myxoma virus expressing feline calicivirus capsid protein. Vaccine 20: 2454–2462
35. Mohandas AR, Dales S (1995) Involvement of spicules in the formation of Vaccinia virus envelopes elucidated by a conditional lethal mutant. Virology 214: 494–502
36. Moss B (2001) *Poxviridae*: the viruses and their replication. In: Knipe DM, Howley PM (eds) Fields Virology, 4th edn. Lippincott Williams & Wilkins, Philadelphia, PA, pp 2849–2883
37. Moss B, Ward BM (2001) High-speed mass transit for poxviruses on microtubules. Nat Cell Biol 3: 245–246
38. Nash P, Barrett J, Cao JX, Hota-Mitchell S, Lalani AS, Everett H, Xu XM, Robichaud J, Hnatiuk S, Ainslie C, Seet BT, McFadden G (1999) Immunomodulation by viruses: the myxoma virus story. Immunol Rev 168: 103–120
39. Ochs M, Fehrenbach H, Richter J (1994) Electron Spectroscopic Imaging (ESI) and Electron Energy Loss Spectroscopy (EELS) of multilamellar bodies and multilamellar body-like structures in tannic acid-treated alveolar septal cells. J Histochem Cytochem 42: 805–809

40. Pieters J (2001) Entry and survival of pathogenic mycobacteria in macrophages. Microb Infect 3: 249–255
41. Purcell DA, Clarke JK (1972) Some aspects of the morphogenesis of Myxoma virus in vivo. Arch Gesamte Virusforsch 39: 369–375
42. Reynolds ES (1963) The use of lead citrate at high pH as an electron-opaque stain in electron microscopy. J Cell Biol 17: 208–212
43. Rietdorf J, Ploubidou A, Reckmann I, Holmstrom A, Frischknecht F, Zettl M, Zimmermann T, Way M (2001) Kinesin-dependent movement on microtubules precedes actin-based motility of vaccinia virus. Nat Cell Biol 3: 992–1000
44. Risco C, Rodriguez JR, Lopez-Iglesias C, Carrascosa JL, Esteban M, Rodriguez D (2002) Endoplasmic reticulum-Golgi intermediate compartment membranes and vimentin filaments participate in vaccinia virus assembly. J Virol 76: 1839–1855
45. Röttger S, Frischknecht F, Reckmann I, Smith GL, Way M (1999) Interactions between vaccinia virus IEV membrane proteins and their roles in IEV assembly and actin tail formation. J Virol 73: 2863–2875
46. Schmelz M, Sodeik B, Ericsson M, Wolffe EJ, Shida H, Hiller G, Griffiths G (1994) Assembly of vaccinia virus: the second wrapping cisterna is derived from the Trans Golgi Network. J Virol 68: 130–147
47. Schrijvers AH, Frederik PM, Stuart MC, Burger KN, Heijnen VV, Van der Vusse GJ, Reneman RS (1989) Formation of multilamellar vesicles by addition of tannic acid to phosphatidylcholine-containing small unilamellar vesicles. J Histochem Cytochem 37: 1635–1643
48. Sieczkarski SB, Whittaker GR (2002) Dissecting virus entry via endocytosis. J Gen Virol 83: 1535–1545
49. Smith GL, Vanderplasschen A, Law M (2002) The formation and function of extracellular enveloped vaccinia virus. J Gen Virol 83: 2915–2931
50. Smith GL, Murphy BJ, Law M (2003) Vaccinia virus motility. Annu Rev Microbiol 57: 323–342
51. Sodeik B, Doms RW, Ericsson M, Hiller G, Machamer CE, van't Hof W, van Meer G, Moss B, Griffiths G (1993) Assembly of vaccinia virus: role of the intermediate compartment between the endoplasmic reticulum and the Golgi stacks. J Cell Biol 121: 521–541
52. Sodeik B, Krijnse-Locker J (2002) Assembly of vaccinia virus revisited: *de novo* membrane synthesis or acquisition from the host? Trends Microbiol 10: 15–24
53. Stoltz DB, Summers MD (1972) Observations on the morphogenesis and structure of a hemocytic poxvirus in the midge *Chironomus attenuatus*. J Ultrastruct Res 40: 581–598
54. Tektoff J, Gazzolo L, Leftheriotis E (1971) Morphogenèse du virus de la myxomatose du lapin. Path Biol 19: 1045–1054
55. Thomas JA, Henry M, Hollande E, Lambre C (1972) Rôle de l'ergastoplasme dans le cycle morphogénétique du virus d'une souche de myxomatose. C R Acad Sci Hebd Seances Acad Sci 275: 3047–3052
56. Tilney LG, Portnoy DA (1989) Actin filaments and the growth, movement, and spread of the intracellular bacterial parasite, *Listeria monocytogenes*. J Cell Biol 109: 1597–1608
57. Traktman P, Liu K, DeMasi J, Rollins R, Jesty S, Unger B (2000) Elucidating the essential role of the A14 phosphoprotein in vaccinia virus morphogenesis: construction and characterization of a tetracycline-inducible recombinant. J Virol 74: 3682–3695

58. Van Eijl H, Hollinshead M, Rodger G, Zhang WH, Smith GL (2002) The Vaccinia virus F12L protein is associated with intracellular enveloped virus particles and is required for their egress to the cell surface. J Gen Virol 83: 195–207
59. Vanderplasschen A, Hollinshead M, Smith GL (1998) Intracellular and extracellular vaccinia virions enter cells by different mechanisms. J Gen Virol 79: 877–887
60. Ward BM, Moss B (2001) Vaccinia virus intracellular movement is associated with microtubules and independent of actin tails. J Virol 75: 11651–11663

Author's address: Dr. Stéphane Bertagnoli, UMR 1225, Ecole Nationale Vétérinaire de Toulouse, 23 chemin des Capelles, BP87614, 31076 Toulouse cedex 03, France; e-mail: s.bertagnoli@envt.fr